

A three-level multi-continua upscaling method for flow problems in fractured porous media

Maria Vasilyeva ^{*} Eric T. Chung [†] Yalchin Efendiev [‡] Aleksey Tyrylgin [§]

October 4, 2018

Abstract

Traditional two level upscaling techniques suffer from a high offline cost when the coarse grid size is much larger than the fine grid size. Thus, multilevel methods are desirable for problems with complex heterogeneities and high contrast. In this paper, we propose a novel three-level upscaling method for flow problems in fractured porous media. Our method starts with a fine grid discretization for the system involving fractured porous media. In the next step, based on the fine grid model, we construct a nonlocal multi-continua upscaling (NLMC) method using an intermediate grid. The system resulting from NLMC gives solutions that have physical meaning. In order to enhance locality, the grid size of the intermediate grid needs to be relatively small, and this motivates using such an intermediate grid. However, the resulting NLMC upscaled system has a relatively large dimension. This motivates a further step of dimension reduction. In particular, we will apply the idea of the Generalized Multiscale Finite Element Method (GMsFEM) to the NLMC system to obtain a final reduced model. We present simulation results for a two-dimensional model problem with a large number of fractures using the proposed three-level method.

1 Introduction

A fast and accurate solution of flow problems in fractured porous media is an important component in reservoir simulations. Direct numerical simulation requires using a very fine grid that resolves all scales and heterogeneities. The resulting discrete formulation on the fine grid leads to a very large system of equations that is computationally expensive to solve. To reduce the dimension of the system, multiscale methods or

^{*}Institute for Scientific Computation, Texas A&M University, College Station, TX 77843-3368 & Department of Computational Technologies, North-Eastern Federal University, Yakutsk, Republic of Sakha (Yakutia), Russia, 677980. Email: vasilyevadotmdotv@gmail.com.

[†]Department of Mathematics, The Chinese University of Hong Kong (CUHK), Hong Kong SAR. Email: tschung@math.cuhk.edu.hk.

[‡]Department of Mathematics & Institute for Scientific Computation (ISC), Texas A&M University, College Station, Texas, USA. Email: efendiev@math.tamu.edu.

[§]Multiscale model reduction laboratory, North-Eastern Federal University, Yakutsk, Republic of Sakha (Yakutia), Russia, 677980.

upsampling techniques are necessary [19, 15, 32, 26, 20]. We will, in this paper, focus on a class of multiscale methods based on local multiscale basis functions. In typical two level methods, multiscale basis functions are constructed locally, namely, within a coarse block or a union of several coarse blocks of an underlying coarse mesh, which does not necessarily resolve any scale. Constructing multiscale basis functions involves solutions, using the fine grid, of some local problems, which can be expensive for the case when coarse grid size is much larger than the fine grid size [9]. Therefore, problems with very large disparate scales require some coarsening techniques or multilevel techniques [21]. The commonly used techniques for such problems are the re-iterated homogenization methods or multilevel multiscale methods [3, 22, 33, 28, 23, 21, 9]. In multilevel multiscale approaches, multiple levels of coarsening are constructed by a recursive application of the basic two level method with the aim of improving computational efficiency. The main advantage of multilevel methods is to avoid solving local problems of large dimensions.

In our previous works, we developed multiscale model reduction techniques based on the Generalized Multiscale Finite Element Method (GMsFEM) for flow in fractured porous media [2, 7, 16, 1]. The general idea of GMsFEM is to design suitable spectral problems on some snapshot spaces to obtain dominant modes of the solutions. These dominant modes are used to construct the required multiscale basis functions [13, 14, 6, 5]. The resulting multiscale space contains basis functions that take into account the microscale heterogeneities as well as high contrast and channelized effects, and the resulting multiscale scale solution provides an accurate and efficient approximation of the fine scale solution. We remark that the GMsFEM is related to the Proper Orthogonal Decomposition (POD) (c.f. [14]) in the way that the GMsFEM constructs multiscale basis functions that optimize an appropriate error within a finite dimensional space. The error of the GMsFEM has a spectral decay and is inversely proportional to the eigenvalues of the spectral problems used for constructing basis functions.

Recently, the authors in [8, 10] proposed a new Constraint Energy Minimizing GMsFEM (CEM-GMsFEM) with the aim of finding a multiscale method with a coarse mesh dependent convergence. Constructing the multiscale space starts with an auxiliary space, which consists of eigenfunctions of a local spectral problem, and is defined for each coarse element. Using the auxiliary space, one can obtain the required multiscale basis functions by solving a constraint energy minimization problem. The resulting multiscale basis functions have an exponential decay away from the coarse element for which the basis functions are formulated. Therefore, the multiscale basis functions are only numerically computed in an oversampled region defined by enlarging the target coarse element by a few coarse layers. It has been shown that these basis functions are able to capture high contrast channel effects. Moreover, the convergence of this method depends only on the coarse grid size, and is independent of the scales and the heterogeneities of the coefficients of the PDE. We remark that the size of the oversampling domains depends on the coarse grid size and depends logarithmically on the contrast of the medium. Recently in [10], we introduced a non-local multi-continuum (NLMC) method for problems in heterogeneous fractured media. In the NLMC method, we construct multiscale basis functions based on the solution of some local constrained energy minimization problems as in the CEM-GMsFEM. One key ingredient of the NLMC method is that we can specify the location of all continua within coarse elements, and we construct these multiscale basis functions so that they have mean value zero in all continua within all coarse elements, except one target continuum within a fixed coarse element. In this case, the

degrees of freedoms of the resulting upscaled system have a physical meaning, namely, they are the mean value of the solution on each continuum within each coarse element. The NLMC has similar theoretical properties as that of the CEM-GMsFEM.

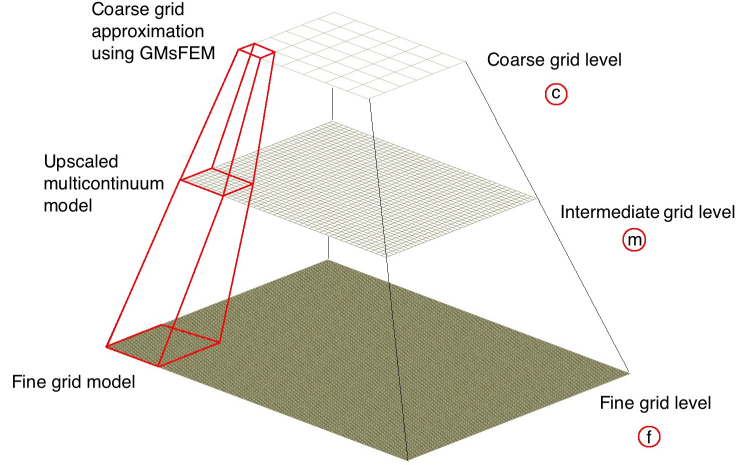


Figure 1: Concept of three-level scheme.

As we mentioned above, two level multiscale methods can still suffer from large offline computational costs. In this work, we propose a new three level multiscale method based on both the GmsFEM and the NLMC with the aim of taking advantage of both methodologies. Overall speaking, the proposed technique is the three-level scheme (see Figure 1) described as follows:

- fine grid model for fractured porous media,
- intermediate grid model based on the NLMC method,
- coarse grid approximation using the GmsFEM.

Our method starts with a fine grid discretization for the system involving fractured porous media. In the next step, based on the fine grid model, we construct an NLMC method using an intermediate grid. As discussed before, the system resulting from the NLMC method gives solutions that have physical meaning, namely, mean values on local continua. We remark that by an intermediate grid, we mean that the grid size is between the fine and the coarse grids. In order to enhance locality, the grid size of the intermediate grid needs to be relatively small, and this motivates using such an intermediate grid. However, the resulting NLMC upscaled system has a relatively large dimension. This motivates a further step of dimension reduction. In particular, we will apply the idea of GmsFEM to the NLMC system to obtain a final reduced model.

This paper contains several novel ideas. We present an extension of the GmsFEM for the NLMC models and show that the GmsFEM can work with any multicontinuum upscaled model. The NLMC method provides an accurate upscaled multicontinuum approximation that we use for intermediate grid approximation. The second advantage of the proposed method is the acceleration of the GmsFEM model construction, when

the solution of the local spectral problems are computationally expensive due to disparate scales and this requires coarsening [9, 21]. Coarsening techniques should provide accurate and fast intermediate grid approximation. For this purpose, the NLMC method is applied for constructing the accurate upscaled intermediate grid model.

The paper is organized as follows. In Section 2, we consider a fine grid model to approximate the flow problem in the fractures porous media. In Section 3, we discuss an intermediate grid upscaled model construction using the NLMC method. Next, we present a construction of the multiscale basis functions on an intermediate grid for the GMsFEM in Section 4 to obtain the final reduced model. Finally, we present numerical results and a conclusion in Section 5.

2 Fine grid model

First, we discuss the fine grid discretization of the flow system. We consider a mixed dimensional mathematical model for flow problem in fractured porous media. A common approach to model fracture media is to consider the fractures as lower-dimensional objects [27, 12, 17, 11]. Let $\Omega \in \mathcal{R}^d$ ($d = 2, 3$) be the computational domain for the porous medium and $\gamma \in \mathcal{R}^{d-1}$ be a reduced dimensional domain representing fracture networks. The flow model can be described as follows

$$\begin{aligned} a_m \frac{\partial p_m}{\partial t} - \nabla \cdot (b_m \nabla p_m) + \eta_m \sigma(p_m - p_f) &= q_m, \quad x \in \Omega, \\ a_f \frac{\partial p_f}{\partial t} - \nabla \cdot (b_f \nabla p_f) - \eta_f \sigma(p_m - p_f) &= q_f, \quad x \in \gamma, \\ a_m &= c_m, \quad a_f = d c_f, \quad b_m = k_m / \mu, \quad b_f = d k_f / \mu, \end{aligned} \quad (1)$$

where μ is the fluid viscosity, c_α , k_α are the compressibility and permeability for porous matrix ($\alpha = m$) and fractured ($\alpha = f$), q_α is the source term for $\alpha = f, m$, d is the fracture thickness, p_m is the pressure in the porous matrix denoted by Ω , p_f is the pressure in the fractures γ . Coefficients η_m and η_f depend on mesh parameters and will be described later.

Let $\mathcal{T}_F = \cup_i \varsigma_i$ be the fine grid with triangular or tetrahedral cells for the domain Ω . The fracture mesh, denoted by $\mathcal{E}_\gamma = \cup_l \iota_l$, is constructed on the fractures domain γ . The coupled system (1) is discretized using the embedded fracture model (EFM) [18, 30, 29]. For the approximation in space, we apply the cell-centered finite-volume method with two-point flux approximation [18, 30, 4, 31, 29]. Thus, we obtain the following discrete problem

$$\begin{aligned} a_m \frac{p_{m,i}^{n+1} - p_{m,i}^n}{\tau} |\varsigma_i| + \sum_j T_{ij} (p_{m,i}^{n+1} - p_{m,j}^{n+1}) + \sigma_{il} (p_{m,i}^{n+1} - p_{f,l}^{n+1}) &= q_m |\varsigma_i|, \quad \forall i = 1, N_F^m, \\ a_f \frac{p_{f,l}^{n+1} - p_{f,l}^n}{\tau} |\iota_l| + \sum_n W_{ln} (p_{f,l}^{n+1} - p_{f,n}^{n+1}) - \sigma_{il} (p_{m,i}^{n+1} - p_{f,l}^{n+1}) &= q_f |\iota_l|, \quad \forall l = 1, N_F^f, \end{aligned} \quad (2)$$

where $T_{ij} = b_m |E_{ij}| / \Delta_{ij}$ ($|E_{ij}|$ is the length of facet between cells ς_i and ς_j , Δ_{ij} is the distance between midpoint of cells ς_i and ς_j), $W_{ln} = b_f / \Delta_{ln}$ (Δ_{ln} is the distance between points l and n), N_F^m is the number of cells in \mathcal{T}_F , N_F^f is the number of cells related to the fracture mesh \mathcal{E}_γ , $\sigma_{il} = \sigma$ if $\iota_l \subset \varsigma_i$ and is zero otherwise.

Here, we choose $\eta_m = 1/|\varsigma_i|$, $\eta_f = 1/|\iota_l|$ and use an implicit scheme for the time discretization, where n is the number of time steps and τ is the given time step size.

We can write the above scheme as the following system of equations for $p^n = (p_m^n, p_f^n)^T$ in matrix form

$$M \frac{p^n - p^{n-1}}{\tau} + Ap^n = F, \quad (3)$$

where

$$M = \begin{pmatrix} M_m & 0 \\ 0 & M_f \end{pmatrix}, \quad A = \begin{pmatrix} A_m + Q & -Q \\ -Q & A_f + Q \end{pmatrix}, \quad F = \begin{pmatrix} F_m \\ F_f \end{pmatrix},$$

and

$$M_m = \{m_{ij}^m\}, \quad m_{ij}^m = \begin{cases} a_m |\varsigma_i| & i = j, \\ 0 & i \neq j \end{cases}, \quad M_f = \{m_{ln}^f\}, \quad m_{ln}^f = \begin{cases} a_f |\iota_l| & l = n, \\ 0 & l \neq n \end{cases},$$

$$Q = \{q_{il}\}, \quad q_{il} = \begin{cases} \sigma & i = l, \\ 0 & i \neq l \end{cases},$$

where $A_m = \{T_{ij}\}$, $A_f = \{W_{ln}\}$, $F_m = \{f_i^m\}$, $f_i^m = q_m |\varsigma_i|$, $F_f = \{f_l^f\}$, $f_l^f = q_f |\iota_l|$. We note that the size of this fine-grid system is $N_F = N_F^m + N_F^f$.

3 The NLMC on intermediate grid

In this section, we will construct an upscaled system for the fine system (3) on an intermediate grid. In particular, we will construct an upscaled model using the nonlocal multicontinua (NLMC) upscaling approach [10]. In this method, the upscaled coefficients are based on the construction of multiscale basis functions. To do so, we solve local problems in some oversample local regions subject to the constraints that the mean values of the local solution vanishes in all continua except the one for which it is formulated. It has been shown that these multiscale basis functions have a spatial decay property and separate background medium and fractures. For more details in the derivation, we refer the reader to [10]. Below, we will state a brief discussion of the derivation.

Let $\mathcal{T}_I = \cup_i K_i$ be a structured intermediate grid. We consider a coarse cell K_i and let K_i^+ be its oversampling region obtained by enlarging K_i with few coarse cell layers. For the fractures, we write $\gamma = \cup_{l=1}^L \gamma^{(l)}$, where $\gamma^{(l)}$ denotes the l -th fracture network and L is the total number of fracture networks. Let $\gamma_j^{(l)} = K_j \cap \gamma^{(l)}$ be the fracture inside cell $K_j \in K_i^+$ and L_j be the number of fractures in K_j . For each $K_j \subset K_i^+$, we therefore need $L_j + 1$ basis functions: one for K_j and one for each $\gamma_j^{(l)}$. Following the framework of [10] and [8], we will construct the required multiscale basis functions by solving a local problem on K_i^+ subject to some constraints to be specified in the following paragraph.

We now define the constraints that will be used for multiscale basis construction. We use $\phi^{i,0}$ to denote the basis function corresponding to the porous matrix in the coarse element K_i and use $\phi^{i,l}$ to denote the basis function corresponding to the l -th continuum within the coarse element K_i . We remark that these basis functions are supported in K_i^+ and have zero trace on ∂K_i^+ . The required constraints are defined as

follows:

(1) porous matrix in K_i , $\phi^{i,0} = (\phi_m^{i,0}, \phi_f^{i,0})$:

$$\int_{K_j} \phi_m^{i,0} dx = \delta_{i,j}, \quad \int_{\gamma_j^{(l)}} \phi_f^{i,0} ds = 0, \quad l = \overline{1, L_j}.$$

(2) l -th fracture network in K_i , $\phi^{i,l} = (\phi_m^{i,l}, \phi_f^{i,l})$:

$$\int_{K_j} \phi_m^{i,l} dx = 0, \quad \int_{\gamma_j^{(l)}} \phi_f^{i,l} ds = \delta_{i,j} \delta_{m,l}, \quad l = \overline{1, L_j}.$$

We remark that the constraints are defined for each $K_j \subset K_i^+$.

To construct the multiscale basis functions with the energy minimizing property, we solve the following local problems in K_i^+ using a fine-grid approximation for flow in fractured porous media presented in Section 2. In particular, we solve the following coupled system in K_i^+ :

$$\begin{pmatrix} A_m^{i,+} + Q^{i,+} & -Q^{i,+} & B_m^T & 0 \\ -Q^{i,+} & A_f^{i,+} + Q^{i,+} & 0 & B_f^T \\ B_m & 0 & 0 & 0 \\ 0 & B_f & 0 & 0 \end{pmatrix} \begin{pmatrix} \phi_m \\ \phi_f \\ \mu_m \\ \mu_f \end{pmatrix} = \begin{pmatrix} 0 \\ 0 \\ G_m \\ G_f \end{pmatrix} \quad (4)$$

with the zero Dirichlet boundary condition on ∂K_i^+ for both ϕ_m and ϕ_f . Here $A_m^{i,+}$, $A_f^{i,+}$ and $Q^{i,+}$ denote the parts of the fine-scale matrices that are related to the local domain K_i^+ . Note that we used Lagrange multipliers μ_m and μ_f to impose the constraints defined above.

For the construction of the multiscale basis function with respect to porous matrix $\phi^{i,0} = (\phi_m^{i,0}, \phi_f^{i,0})$, we set $G_m = \delta_{i,j}$ and $G_f = 0$. For the multiscale basis function $\phi^{i,l} = (\phi_m^{i,l}, \phi_f^{i,l})$ with respect to the l -th fracture network, we set $G_m = 0$ and $G_f = \delta_{i,j} \delta_{m,l}$. Combining these multiscale basis functions, we obtain the following multiscale space

$$V_{ms} = \text{span}\{(\phi_m^{i,l}, \phi_f^{i,l}), i = \overline{1, N_c}, l = \overline{0, L_i}\}$$

and the projection matrix

$$R = \begin{pmatrix} R_{mm} & R_{mf} \\ R_{fm} & R_{ff} \end{pmatrix},$$

where

$$\begin{aligned} R_{mm}^T &= [\phi_m^{0,0}, \phi_m^{1,0} \dots \phi_m^{N_c,0}], \quad R_{ff}^T = [\phi_f^{0,1} \dots \phi_f^{0,L_0}, \phi_f^{1,1} \dots \phi_f^{1,L_1}, \dots, \phi_f^{N_c,1} \dots \phi_f^{N_c,L_{N_c}}], \\ R_{mf}^T &= [\phi_f^{0,0}, \phi_f^{1,0} \dots \phi_f^{N_c,0}], \quad R_{fm}^T = [\phi_m^{0,1} \dots \phi_m^{0,L_0}, \phi_m^{1,1} \dots \phi_m^{1,L_1}, \dots, \phi_m^{N_c,1} \dots \phi_m^{N_c,L_{N_c}}], \end{aligned}$$

Finally, the resulting upscaled intermediate grid model reads

$$\bar{M} \frac{\bar{p}^n - \bar{p}^{n-1}}{\tau} + \bar{A} \bar{p}^n = \bar{F}, \quad (5)$$

where $\bar{A} = RAR^T$, $\bar{p} = (\bar{p}_m, \bar{p}_f)$ is the average cell solution on intermediate grid element for porous matrix (\bar{p}_m) and for fractures (\bar{p}_f). We can reconstruct the downscale solution by $p = R^T \bar{p}$.

As an approximation, we use diagonal mass matrix directly calculated on the intermediate grid

$$\bar{M} = \begin{pmatrix} \bar{M}_m & 0 \\ 0 & \bar{M}_f \end{pmatrix}, \quad \bar{F} = \begin{pmatrix} \bar{F}_m \\ \bar{F}_f \end{pmatrix},$$

where $\bar{M}_m = \text{diag}\{a_m|K_i|\}$, $\bar{M}_f = \text{diag}\{a_f|\gamma_i|\}$, and for the right-hand side vector $\bar{F}_m = \{q_m|K_i|\}$, $\bar{F}_f = \{q_f|\gamma_i|\}$. We remark that the matrix A is non-local and provides a good approximation due to the coupling of various components in the basis construction. The resulting upscaled model has one degree of freedom (DOF) for each fracture network and the size of intermediate grid system is $N_I = N_{cell}^I + \sum_{i=1}^{N_{cell}^I} L_i$, where N_{cell}^I is the number of intermediate grid cells.

4 The GMsFEM on coarse grid

In this section, we will present a model reduction technique based on the GMsFEM. We will form a reduced model on a coarse grid based on the NLMC system constructed in the previous section. Generally speaking, the GMsFEM is a systematic approach to identify multiscale basis functions via local spectral problems [14, 13]. In the original GMsFEM, the method is constructed based on a fine grid discretization of the PDE. In this paper, we will apply the GMsFEM idea to the system resulting from the NLMC method and this is a new idea. To obtain a reduced system using GMsFEM, we first identify the local matrices from the NLMC system corresponding to a set of overlapping coarse regions, typically called coarse neighborhoods [14]. Then for each coarse neighborhood, we solve a spectral problem using the local matrices, and select the dominant eigenfunctions corresponding to the small eigenvalues. The multiscale basis functions are then obtained by multiplying a suitable partition of unity function to the eigenfunctions. Finally, the GMsFEM system is obtained by forming a suitable projection matrix using the basis functions.

For completeness, we summarize below the main steps in GMsFEM:

Preprocessing (offline stage).

- The construction of the multiscale basis functions in local domains.
- The construction of the coarse grid system.

Solver (online stage).

- Solution of the coarse grid system.

Postprocessing.

- Reconstruction of the fine grid solution.

In the following, we will describe the construction of the multiscale basis functions ψ_k^ω which is supported in a coarse neighborhood ω , where k represents the numbering of the basis functions.

Let $\mathcal{T}_C = \cup_i \Theta_i$ be the structured coarse grid and assume that each coarse element is a connected union of fine grid and intermediate grid blocks. We use $\{x_i\}_{i=1}^{N_{vert}^C}$ to denote the vertices of the coarse mesh

\mathcal{T}_C , where N_{vert}^C is the number of coarse nodes. We define the coarse neighborhood of the node x_i by $\omega_i = \cup_j \{\Theta_j | x_i \in \bar{\Theta}_j\}$.

We now consider a coarse neighborhood ω_i . In order to construct the multiscale space $V_{ms}^{\omega_i}$ with respect to ω_i , we solve following local spectral problem in local domain ω_i

$$A\Psi^i = \lambda^i S\Psi^i, \quad (6)$$

where the matrix A is the restriction of the matrix \bar{A} in the coarse neighborhood ω_i and the matrix \bar{A} is the matrix resulting from the NLMC method (5). Moreover, the matrix S is defined as follows:

$$S = \begin{pmatrix} \bar{S}_m & 0 \\ 0 & \bar{S}_f \end{pmatrix}, \quad \bar{S}_m = \{s_{ij}^m\}, \quad s_{ij}^m = \begin{cases} b_m |K_i| & i = j, \\ 0 & i \neq j \end{cases}, \quad \bar{S}_f = \{s_{ln}^f\}, \quad s_{ln}^f = \begin{cases} b_f |\gamma_l| & l = n, \\ 0 & l \neq n \end{cases}.$$

To define the required multiscale space, we choose eigenvectors Ψ_k^i ($k = 1, \dots, M_i$) corresponding to the smallest M_i eigenvalues and set

$$V_C = \text{span}\{\psi_k^i = \chi_i \Psi_k^i : 1 \leq i \leq N_{vert}^C \text{ and } 1 \leq k \leq M_i\}, \quad (7)$$

where χ_i are the standard linear partition of unity functions and M_i denotes the number of eigenvectors that are chosen for each coarse node i . The construction in (7) yields a counterpart of the continuous basis functions due to the multiplication of local domain eigenvectors with the continuous partition of unity functions.

Using a single index notation for the basis functions, we may write

$$V_C = \text{span}\{\psi_1, \psi_2, \dots, \psi_{N_C}\}, \quad R_C^T = [\psi_1, \dots, \psi_{N_C}],$$

where R_C is the projection matrix and $N_C = \sum_{i=1}^{N_{vert}^C} M_i$ is the size of the coarse grid system. Finally, we can write the GmsFEM system as

$$M_C \frac{p_C^n - p_C^{n-1}}{\tau} + A_C p_C^n = F_C, \quad (8)$$

and $p_C \in V_C$ and $p_C = \sum_i p_{C,i} \psi_i(x)$. In the above system, we have

$$M_C = R_C \bar{M} R_C^T, \quad A_C = R_C \bar{A} R_C^T, \quad F_C = R_C \bar{F},$$

and $\bar{p} = R_C^T p_C$ is the reconstructed intermediate grid solution and $p = R^T \bar{p}$ is the reconstructed fine grid solution.

5 Numerical results

In this section, we present numerical results for our three level scheme. We consider the problem in domain $\Omega = [0, 1] \times [0, 1]$. As model problems, we consider two geometries with different fracture distribution:

- *Geometry 1.* Domain with 30 fracture lines.

- *Geometry 2*. Domain with 160 fracture lines.

In Figure 2, we show computational grids for *Geometry 1* and *Geometry 2*. The implementation is based on the open-source simulation library FEniCS, where we use geometry objects and interface to the linear and spectral solvers [24, 25].

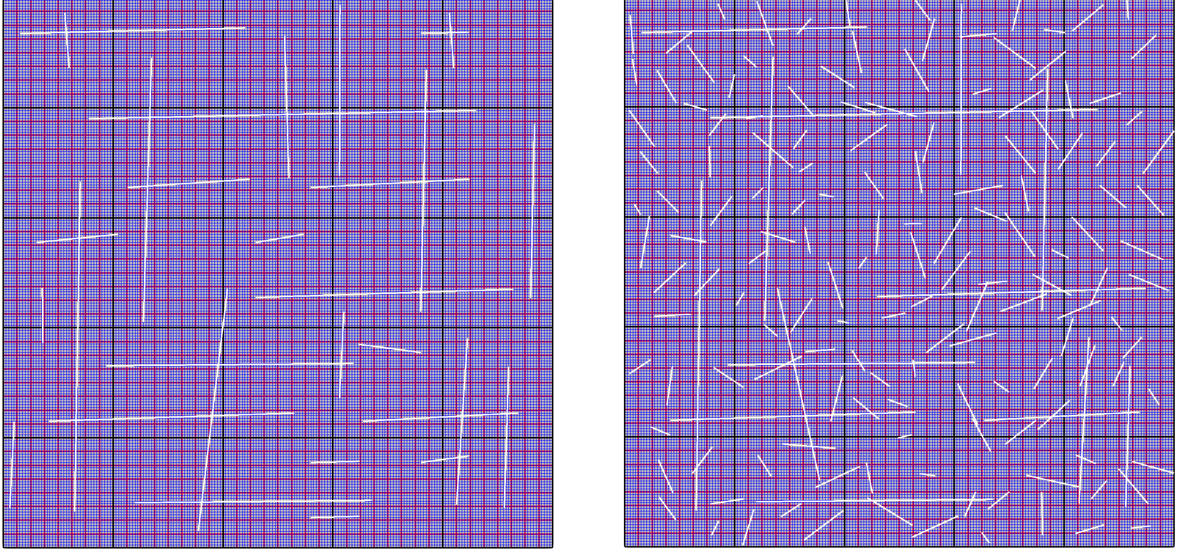


Figure 2: Computational grids (black color - coarse grid, red color - intermediate grid and blue color - fine grid). Fractures are depicted by white color. Left: *Geometry 1* with 30 fracture lines. Right: *Geometry 2* with 160 fracture lines.

s	e_I^{FI}	e_F^{FI}
1	5.466	17.626
2	0.416	3.917
3	0.112	0.901
4	0.103	0.236
6	0.101	0.104

s	e_I^{FI}	e_F^{FI}
1	50.412	51.208
2	1.205	4.177
3	0.385	0.930
4	0.126	0.229
6	0.123	0.228

Table 1: Relative errors for NLMC intermediate grid solution with different number of oversampling layers K^s , $s = 1, 2, 3, 4$ and 6. Left: *Geometry 1* with $DOF_I = 1965$ and $DOF_F = 41042$. Right: *Geometry 2* with $DOF_I = 2428$ and $DOF_F = 43216$.

We construct three grids for multiscale solver:

- *Fine* level with mesh 200×200 .
- *Intermediate* level with mesh 40×40 .

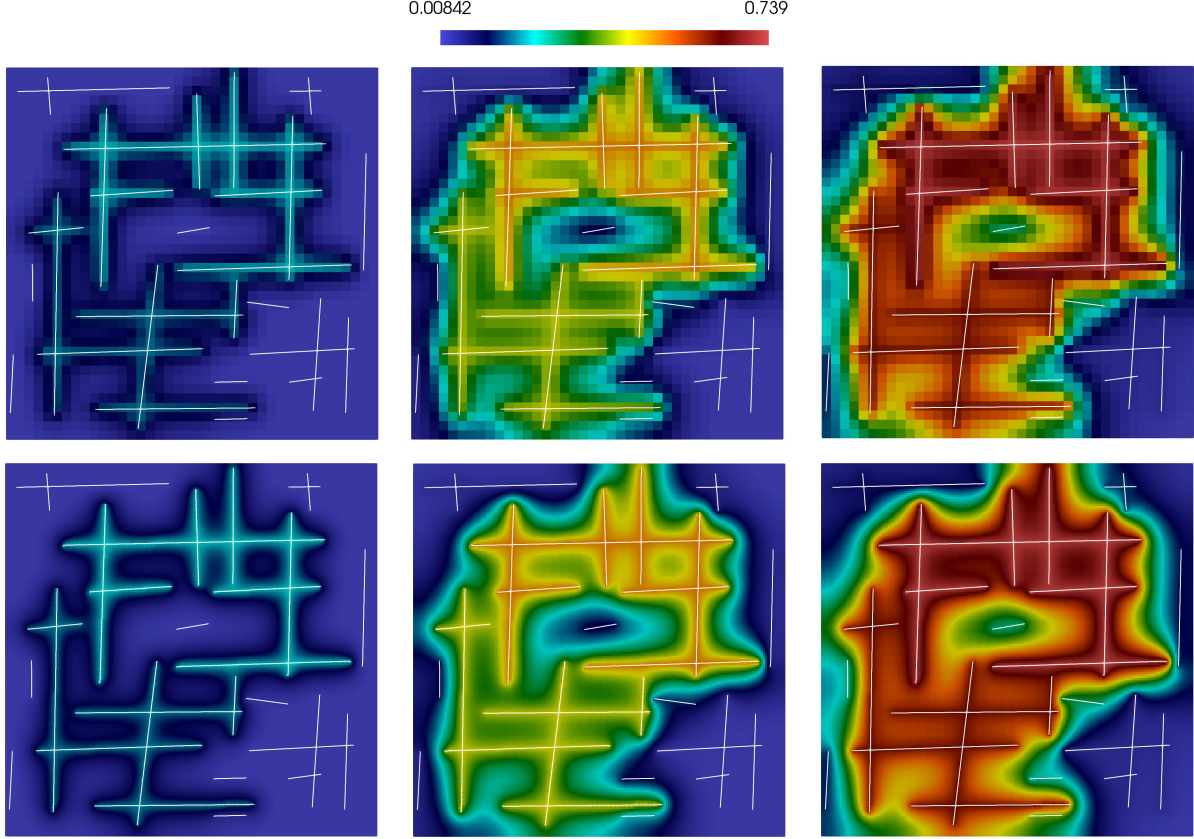


Figure 3: Multiscale solutions on mesh 40×40 with K^4 using NLMC model for different time steps $t_{10} = 0.02$, $t_{30} = 0.06$ and $t_{50} = 0.1$ (from top to bottom). *Geometry 1*. First row: upscaled intermediate grid solution. Second row: downscaled fine grid solution.

- *Coarse* level with coarse grids 5×5 and 10×10 .

For approximation on fine grid, we construct finite volume approximation using embedded fracture model. We note that, another approximation techniques can be used, for example, discrete fracture model with unstructured grids. Fine grid for fractures domain for *Geometry 2* contains 3216 cells. For *Geometry 1*, we use grid with 1042 cells for fractures. In Figure 2, the fine grid for *Geometry 1* and *Geometry 2* is depicted with blue color and contains 40000 cells. The intermediate grid is depicted by red color and contains 1600 cells. By black color, we depict the coarse grid that contains 36 and 121 vertices. Note that DOF_C , DOF_I and DOF_F are the number of degrees of freedom for coarse, intermediate and fine grids approximations.

We set following parameters for model problem: $a_m = 10^{-5}$, $a_f = 10^{-6}$, $b_m = 10^{-6}$, $b_f = 1.0$ with $\sigma = 10^{-4}$. We set $p_0 = 0$ as initial pressure and zero flux on boundary. We set a source term on the fractures inside cells $K = [0.1, 0.15] \times [0.05, 0.1]$ and $K = [0.6, 0.65] \times [0.9, 0.95]$ with $q = 10^{-3}$. We simulate $t_{max} = 0.1$ with 50 time steps.

Intermediate grid approximation using NLMC method.

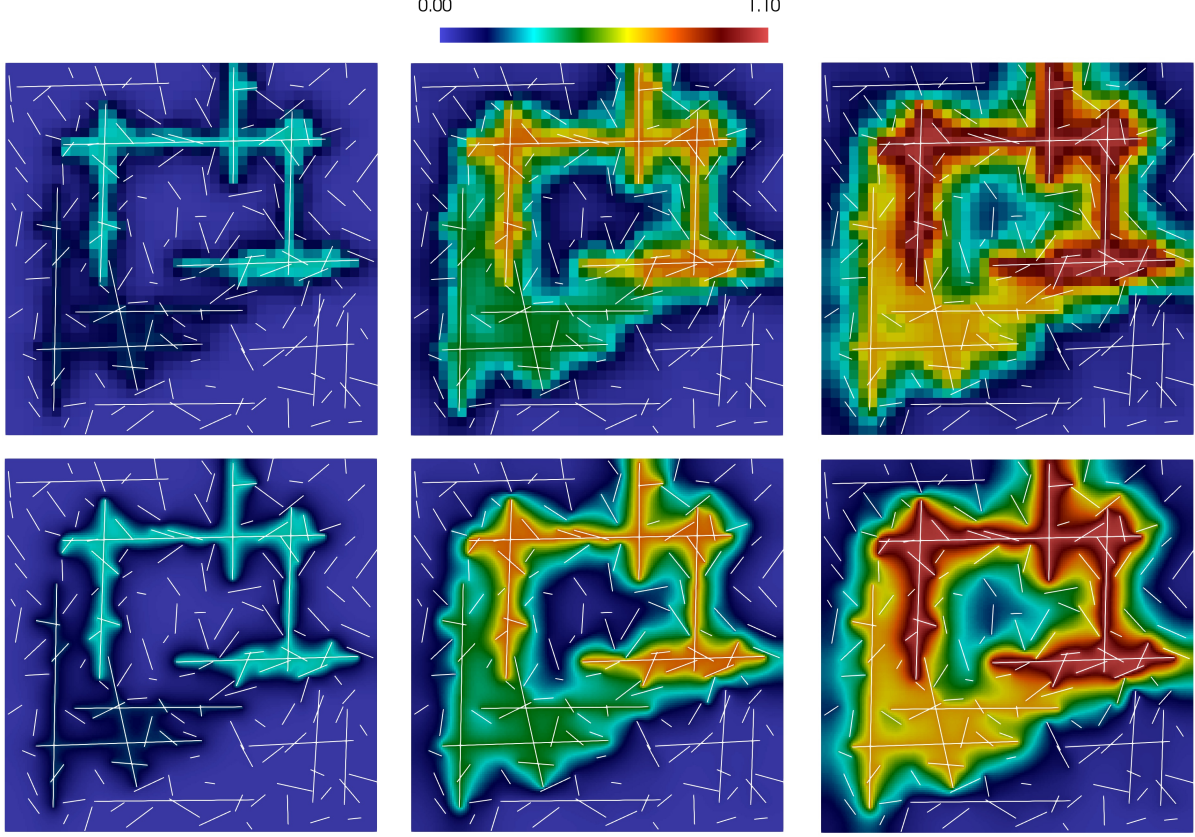


Figure 4: Multiscale solutions on mesh 40×40 with K^4 using NLMC model for different time steps $t_{10} = 0.02$, $t_{30} = 0.06$ and $t_{50} = 0.1$ (from top to bottom). *Geometry 2*. First row: upscaled intermediate grid solution. Second row: downscaled fine grid solution.

First, we consider relative errors for upscaled multicontinuum model using NLMC method on intermediate grid. To compare the results, we use the relative L^2 errors between fine grid in upscaled intermediate grid models e_I^{FI} . We calculate errors on intermediate grid (e_I^{FI}) and on fine grid (e_F^{FI})

$$e_I^{FI} = \frac{\|p_I - \bar{p}\|_{L^2}}{\|p_I\|_{L^2}}, \quad e_F^{FI} = \frac{\|p - \bar{p}_F\|_{L^2}}{\|p\|_{L^2}},$$

where \bar{p} is the upscaled intermediate grid solution, $\bar{p}_F = R^T \bar{p}$ is the downscaled of fine grid intermediate grid solution \bar{p} , p is the reference fine grid solution, p_I is the intermediate grid cell average for reference fine grid solution p and

$$\|p_I - \bar{p}\|_{L^2}^2 = \sum_K (p_I^K - \bar{p}^K)^2, \quad p_I^K = \frac{1}{|K|} \int_K p \, dx.$$

In Figures 3 and 4, we present the pressure on mesh 40×40 with K^4 using upscaled model for different time steps $t_{10} = 0.02$, $t_{30} = 0.06$ and $t_{50} = 0.1$ *Geometry 1* and *Geometry 2*, respectively. In the first row, we depict an upscaled medium grid solution. Using projection matrix, we can reconstruct fine grid solution from intermediate grid upscaled model (second row in figures). The fine-scale systems have $DOF_f = 41042$

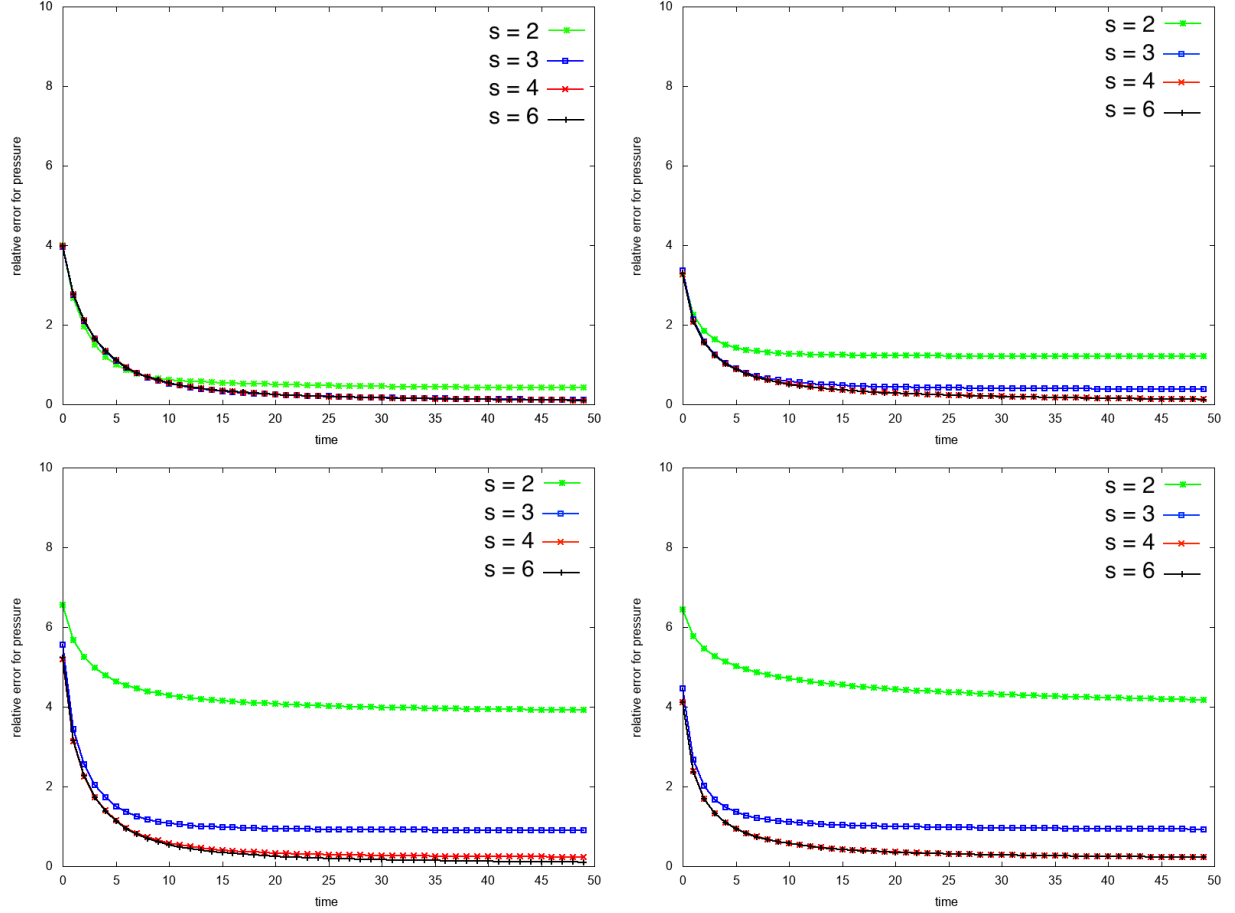


Figure 5: Relative errors vs time for upscaled intermediate grid solution with different number of oversampling layers K^s , $s = 2, 3, 4$ and 6. Left: *Geometry 1*. Right: *Geometry 2*.

for *Geometry 1* and $DOF_f = 43216$ for *Geometry 2*. Upscaled intermediate grid model has $DOF_c = 1965$ for *Geometry 1* and $DOF_c = 2428$ for *Geometry 2*. NLMC method provides accurate meaningful intermediate grid solution with less than one percent errors on fine and intermediate grids.

In Tables 3 and 4, we show relative errors on intermediate and fine grids for different number of oversampling layers K^s with $s = 1, 2, 3, 4$ and 6. For intermediate grid approximation with 1600 cells, when we take 4 oversampling layers, we have 0.1% of intermediate grid error at final time for *Geometry 1* and similar fine grid error. We observe that one oversampling layer cannot provide accurate solution and we should use sufficient number of oversampling layers for obtaining good solution. In Figures 5, we show relative errors vs time for upscaled intermediate and fine grids solution with different number of oversampling layers K^s , $s = 2, 3, 4$ and 6. For intermediate grid solution, we can obtain accurate results with more than 2 oversampling layers. For accurate reconstructed fine grid solution, we should take more than 3 oversampling layers. The proposed method provide accurate solutions for unsteady mixed dimensional coupled system for fractured porous media for both test geometries and reduce size of the system a lot. For example, we

have $DOF_I = 1965$ and $DOF_F = 41042$ for *Geometry 1*. For *Geometry 2*, we have $DOF_I = 2428$ and $DOF_F = 43216$.

M	DOF_C	e_I^{IC}	e_F^{IC}	M	DOF_C	e_I^{IC}	e_F^{IC}
1	36	49.155	49.475	1	36	59.190	59.519
4	144	9.065	10.146	4	144	59.189	59.518
8	288	7.823	8.917	8	288	58.316	58.450
12	432	4.506	5.210	12	432	37.888	37.954
16	576	2.218	2.634	16	576	8.046	8.417
20	720	1.588	1.903	20	720	3.667	4.303
24	864	0.908	1.116	24	864	2.021	2.599
28	1008	0.370	0.503	28	1008	1.934	2.491

Table 2: Relative errors for GMsFEM with 5×5 coarse grid solution with different number of multiscale basis functions M . Left: *Geometry 1*. Right: *Geometry 2*.

M	DOF_C	e_I^{IC}	e_F^{IC}	M	DOF_C	e_I^{IC}	e_F^{IC}
1	121	48.473	48.616	1	121	59.190	59.519
2	242	15.437	16.173	2	242	59.124	59.422
4	484	3.949	4.531	4	484	42.111	41.714
8	968	1.177	1.446	8	968	3.171	3.867
12	1452	0.367	0.495	12	1452	1.336	1.772

Table 3: Relative errors for GMsFEM with 10×10 coarse grid. solution with different number of multiscale basis functions M . Left: *Geometry 1*. Right: *Geometry 2*.

Coarse grid approximation using GMsFEM.

Next, we consider the coarse grid approximation using GMsFEM using intermediate grid upscaled model. We use an intermediate grid approximation projection matrix for reconstruction of the fine grid solution. We calculate errors between reference fine grid and GMsFEM solutions on intermediate and fine grids

$$e_I^{IC} = \frac{\|p_I - p_C\|_{L^2}}{\|p_I\|_{L^2}}, \quad e_F^{IC} = \frac{\|p - p_F\|_{L^2}}{\|p\|_{L^2}},$$

where p_C is the GMsFEM solution, $p_F = R^T p_C$ is the reconstructed fine grid GMsFEM solution, p is the reference fine grid solution, p_I is the intermediate grid cell average for reference fine grid solution p .

We consider two coarse grids: 5×5 and 10×10 . In Tables 2 and 3, we show relative errors on intermediate and fine grids for different number of multiscale basis functions, M . The construction of the multiscale basis functions performed on intermediate grid. For coarse grid approximation with 36 vertices for sufficient number of multiscale basis function, we obtain accurate solution with one percent of errors for *Geometry 1* and *Geometry 2*. For finer coarse grid, we can use smaller number of multiscale basis functions for accurate approximation. In Figures 6 and 7, we depict the relative errors vs time for GMsFEM with 5×5 and 10×10

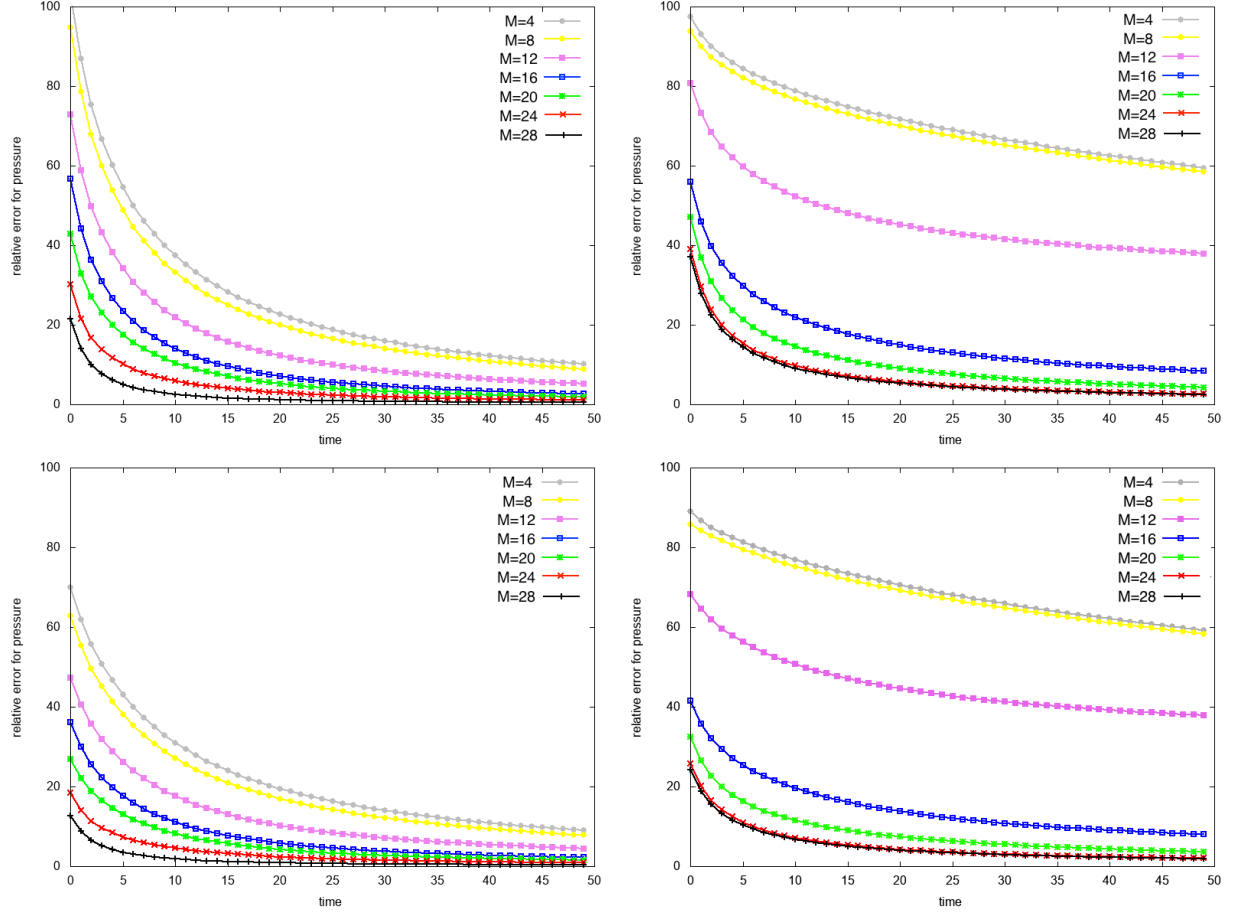


Figure 6: Relative errors vs time for GMsFEM with 5×5 coarse grid. First row: e_I^{IC} . Second row: e_F^{IC} . Left: *Geometry 1*. Right: *Geometry 2*.

coarse grid, respectively. We observe that for geometry with larger number of fractures, we should use more multiscale basis functions. For example, we obtain 3.9% of intermediate grid errors for *Geometry 1*, when we take 4 multiscale basis functions on 10×10 coarse grids. We obtain similar errors for *Geometry 2*, when we take 8 multiscale basis functions.

Finally, we discuss the computational advantages in terms of degrees of freedom. In GMsFEM method, we have offline and online stages. On online stage, we calculate multiscale basis functions and construct coarse grid matrices. On offline stage, we solve coarse grid system. We can consider proposed algorithm as an extension of the GMsFEM for the upscaled multicontinuum models. The advantage of the proposed method in the acceleration of the GMsFEM model construction by performing offline stage on the intermediate coarse grid for upscaled model, where nonlocal multicontinuum method used for construction an accurate model.

Next, we consider the computational advantages of the offline computations. Let N_{vert}^C is the number local domains ω_i , $i = 1, \dots, N_{vert}^C$. We construct multiscale basis functions in each ω by solution of the

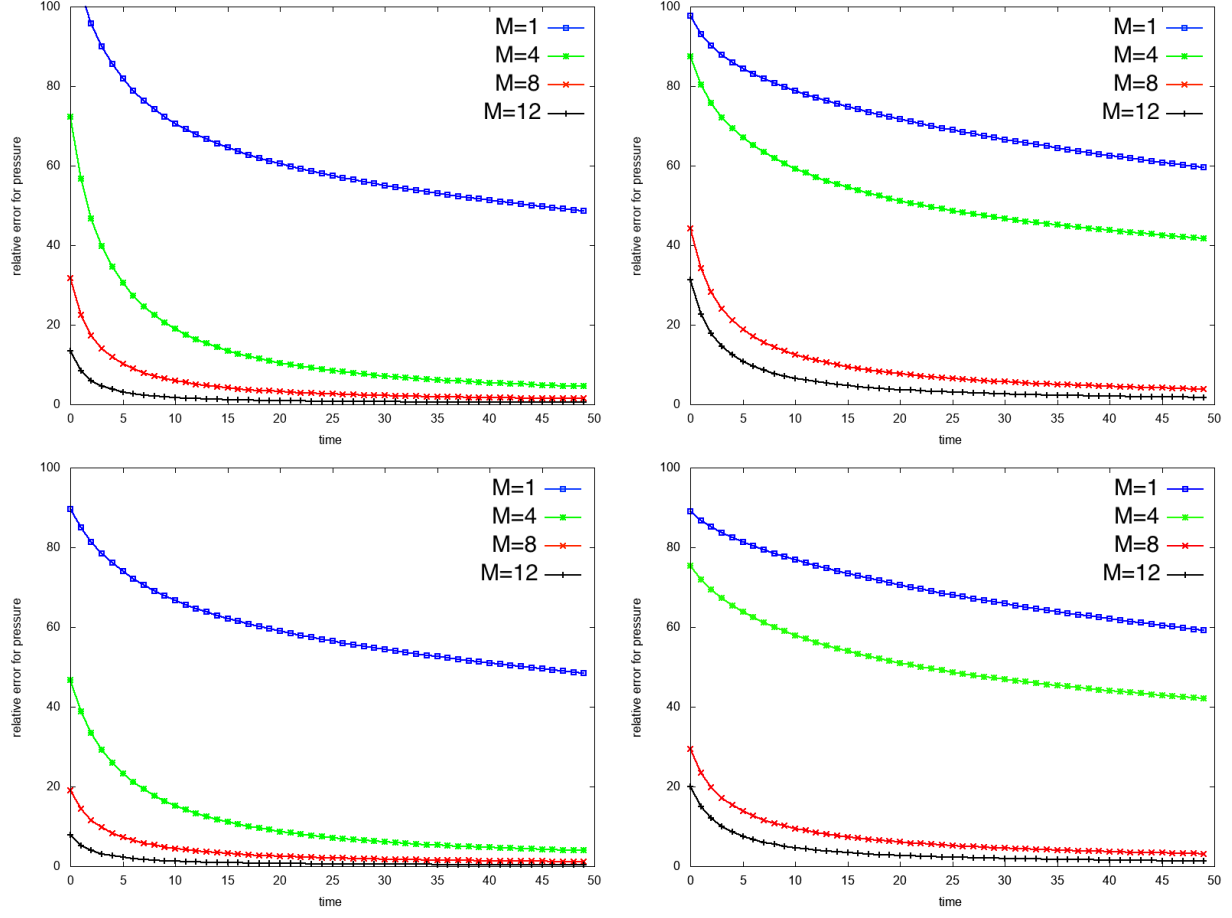


Figure 7: Relative errors vs time for GMsFEM with 10×10 coarse grid. First row: e_I^{IC} . Second row: e_F^{IC} . Left: *Geometry 1*. Right: *Geometry 2*.

local spectral problems. If we perform calculations of the fine grid, the number of degrees of freedom of local spectral problem is $DOF_\omega = N_F^\omega$, where for finite volume approximation $N_F^\omega = N_F^{\omega,m} + N_F^{\omega,f}$, $N_F^{\omega,m}$ and $N_F^{\omega,f}$ is the number of fine grid cells for porous matrix and for fractures grid, respectively. When we perform solution on the local spectral problem on intermediate grid using upscaled model, we have $DOF_\omega = N_{cells}^{I,\omega} + \sum_{j=1}^{N_{cells}^{I,\omega}} L_j$, where $N_{cells}^{I,\omega}$ is the number of intermediate grid cells K_j in ω and L_j^ω is the number of fractures in $K_j \in \omega$. If fine grid is 200×200 and intermediate grid is 40×40 , then for local domain ω_{26} and performing calculations on the fine grid, we have $DOF_\omega = 6899$ with $N_F^{\omega,m} = 6400$ and $N_F^{\omega,f} = 499$ for coarse grid 5×5 . For same coarse grid and same local domain, for the case of intermediate grid based GMsFEM basis construction, we have $DOF_\omega = 387$ with $N_{cells}^{I,\omega} = 256$. Furthermore, construction of the coarse grid system using intermediate upscaled model can also be done much faster. For online computation using GMsFEM on coarse grid 5×5 , we have $DOF_C = 720$ for 20 multiscale basis functions and for fine grid $DOF_F = 41042$ for *Geometry 1*.

We proposed three-level technique for multiscale simulations for fractured porous media. On the fine

grid we use embedded fracture model, but another methods can be used, for example, discrete fracture model. On intermediate grid, we use nonlocal multicontinuum method to construct an upscaled model. On coarse grid, we construct multiscale solver based on the Generalized Multiscale Finite Element Method. We perform numerical simulations for three-level method for model problems for two fractures geometries.

References

- [1] I Yucel Akkutlu, Yalchin Efendiev, Maria Vasilyeva, and Yuhe Wang. Multiscale model reduction for shale gas transport in poroelastic fractured media. *Journal of Computational Physics*, 353:356–376, 2018.
- [2] IY Akkutlu, Yalchin Efendiev, and Maria Vasilyeva. Multiscale model reduction for shale gas transport in fractured media. *Computational Geosciences*, pages 1–21, 2015.
- [3] Alain Bensoussan, Jacques-Louis Lions, and George Papanicolaou. *Asymptotic analysis for periodic structures*, volume 374. American Mathematical Soc., 2011.
- [4] Sebastian Bosma, Hadi Hajibeygi, Matei Tene, and Hamdi A Tchelepi. Multiscale finite volume method for discrete fracture modeling on unstructured grids (ms-dfm). *Journal of Computational Physics*, 2017.
- [5] E. T. Chung, Y. Efendiev, G. Li, and M. Vasilyeva. Generalized multiscale finite element method for problems in perforated heterogeneous domains. *to appear in Applicable Analysis*, 255:1–15, 2015.
- [6] Eric Chung, Yalchin Efendiev, and Thomas Y Hou. Adaptive multiscale model reduction with generalized multiscale finite element methods. *Journal of Computational Physics*, 320:69–95, 2016.
- [7] Eric T Chung, Yalchin Efendiev, Tat Leung, and Maria Vasilyeva. Coupling of multiscale and multi-continuum approaches. *GEM-International Journal on Geomathematics*, 8(1):9–41, 2017.
- [8] Eric T Chung, Yalchin Efendiev, and Wing Tat Leung. Constraint energy minimizing generalized multiscale finite element method. *arXiv preprint arXiv:1704.03193*, 2017.
- [9] Eric T Chung, Yalchin Efendiev, Wing Tat Leung, and Maria Vasilyeva. Reiterated multiscale model reduction using the generalized multiscale finite element method. *International Journal for Multiscale Computational Engineering*, 14(6), 2016.
- [10] Eric T Chung, Yalchin Efendiev, Wing Tat Leung, Yating Wang, and Maria Vasilyeva. Non-local multi-continua upscaling for flows in heterogeneous fractured media. *arXiv preprint arXiv:1708.08379*, 2017.
- [11] Carlo D’angelo and Alfio Quarteroni. On the coupling of 1d and 3d diffusion-reaction equations: application to tissue perfusion problems. *Mathematical Models and Methods in Applied Sciences*, 18(08):1481–1504, 2008.

- [12] Carlo D’Angelo and Anna Scotti. A mixed finite element method for darcy flow in fractured porous media with non-matching grids. *ESAIM: Mathematical Modelling and Numerical Analysis*, 46(2):465–489, 2012.
- [13] Y. Efendiev, J. Galvis, and E. Gildin. Local-global multiscale model reduction for flows in highly heterogeneous media. *Journal of Computational Physics*, 231 (24):8100–8113, 2012.
- [14] Y. Efendiev, J. Galvis, and T. Hou. Generalized multiscale finite element methods. *Journal of Computational Physics*, 251:116–135, 2013.
- [15] Y. Efendiev and T. Hou. *Multiscale Finite Element Methods: Theory and Applications*, volume 4 of *Surveys and Tutorials in the Applied Mathematical Sciences*. Springer, New York, 2009.
- [16] Yalchin Efendiev, Seong Lee, Guanglian Li, Jun Yao, and Na Zhang. Hierarchical multiscale modeling for flows in fractured media using generalized multiscale finite element method. *arXiv preprint arXiv:1502.03828*, 2015. to appear in International Journal on Geomathematics, (DOI) 10.1007/s13137-015-0075-7.
- [17] Luca Formaggia, Alessio Fumagalli, Anna Scotti, and Paolo Ruffo. A reduced model for darcy’s problem in networks of fractures. *ESAIM: Mathematical Modelling and Numerical Analysis*, 48(4):1089–1116, 2014.
- [18] H. Hajibeygi, D. Kavounis, and P. Jenny. A hierarchical fracture model for the iterative multiscale finite volume method. *Journal of Computational Physics*, 230(24):8729–8743, 2011.
- [19] T. Hou and X.H. Wu. A multiscale finite element method for elliptic problems in composite materials and porous media. *J. Comput. Phys.*, 134:169–189, 1997.
- [20] Patrick Jenny, Seong H Lee, and Hamdi A Tchelepi. Adaptive multiscale finite-volume method for multiphase flow and transport in porous media. *Multiscale Modeling & Simulation*, 3(1):50–64, 2005.
- [21] Rouven Künze, Ivan Lunati, and Seong H Lee. A multilevel multiscale finite-volume method. *Journal of Computational Physics*, 255:502–520, 2013.
- [22] Jacques-Louis Lions, Dag Lukkassen, Lars-Erik Persson, and Peter Wall. Reiterated homogenization of nonlinear monotone operators. *Chinese Annals of Mathematics*, 22(01):1–12, 2001.
- [23] Konstantin Lipnikov, J David Moulton, and Daniil Svyatskiy. A multilevel multiscale mimetic (m3) method for two-phase flows in porous media. *Journal of Computational Physics*, 227(14):6727–6753, 2008.
- [24] Anders Logg. Efficient representation of computational meshes. *International Journal of Computational Science and Engineering*, 4(4):283–295, 2009.
- [25] Anders Logg, Kent-Andre Mardal, and Garth Wells. *Automated solution of differential equations by the finite element method: The FEniCS book*, volume 84. Springer Science & Business Media, 2012.

- [26] Ivan Lunati and Patrick Jenny. Multiscale finite-volume method for compressible multiphase flow in porous media. *Journal of Computational Physics*, 216(2):616–636, 2006.
- [27] Vincent Martin, Jérôme Jaffré, and Jean E Roberts. Modeling fractures and barriers as interfaces for flow in porous media. *SIAM Journal on Scientific Computing*, 26(5):1667–1691, 2005.
- [28] Richard Szeliski. Fast surface interpolation using hierarchical basis functions. *IEEE Transactions on Pattern Analysis and Machine Intelligence*, 12(6):513–528, 1990.
- [29] M Tene, MS Al Kobaisi, and H Hajibeygi. Multiscale projection-based embedded discrete fracture modeling approach (f-ams-pedfm). In *ECMOR XV-15th European Conference on the Mathematics of Oil Recovery*, 2016.
- [30] Matei Tene, Mohammed Saad Al Kobaisi, and Hadi Hajibeygi. Algebraic multiscale method for flow in heterogeneous porous media with embedded discrete fractures (f-ams). *Journal of Computational Physics*, 321:819–845, 2016.
- [31] Matei Tene, Sebastian BM Bosma, Mohammed Saad Al Kobaisi, and Hadi Hajibeygi. Projection-based embedded discrete fracture model (pedfm). *Advances in Water Resources*, 105:205–216, 2017.
- [32] E Weinan, Bjorn Engquist, Xiantao Li, Weiqing Ren, and Eric Vanden-Eijnden. Heterogeneous multi-scale methods: a review. *Commun. Comput. Phys*, 2(3):367–450, 2007.
- [33] Zheng Yuan and Jacob Fish. Hierarchical model reduction at multiple scales. *International journal for numerical methods in engineering*, 79(3):314–339, 2009.